ORGANOMETALLICS
Article
Cite This: Organometallics XXXX, XXX, XXX−XXX
pubs.acs.org/Organometallics

Fluoro-imidazopyridinylidene Ruthenium Catalysts for Cross Metathesis with Ethylene

Seunghwan Byun,[†,‡] Huiyeong Seo,[†] Jun-Ho Choi,[†] Ji Yeon Ryu,[§] Junseong Lee,[§] Won-jin Chung,*[,†] and Sukwon Hong*[,†,‡,∥]

[†]Department of Chemistry, Gwangju Institute of Science and Technology, 123 Cheomdan-gwagi-ro, Buk-gu, Gwangju 61005, Republic of Korea

[‡]Grubbs Center for Polymers and Catalysis, Gwangju Institute of Science and Technology, 123 Cheomdan-gwagi-ro, Buk-gu, Gwangju 61005, Republic of Korea

[§]Department of Chemistry, Chonnam National University, 77 Yongbong-ro, Buk-gu, Gwangju 61186, Republic of Korea

[∥]School of Materials Science and Engineering, Gwangju Institute of Science and Technology, 123 Cheomdan-gwagi-ro, Buk-gu, Gwangju 61005, Republic of Korea

Supporting Information

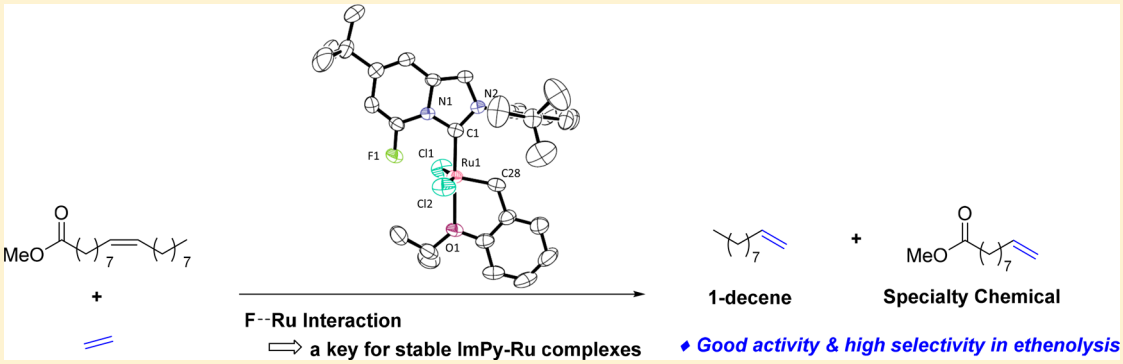

ABSTRACT: A series of ruthenium metathesis catalysts bearing fluorinated imidazo[1,5-*a*]pyridin-3-ylidene carbenes (F-ImPy) were developed for ethenolysis (cross metathesis with ethylene) of methyl oleate. X-ray crystal structure analysis shows Ru−F interaction, and this fluorine substitution appears to be pivotal to have stable ImPy-Ru precatalysts. Ligand structure was varied for high catalyst activity and cross metathesis selectivity in ethenolysis reaction. F-ImPy-Ru catalysts showed high selectivity in ethenolysis of methyl oleate and thermal robustness under an ethylene atmosphere.

INTRODUCTION

Catalytic olefin metathesis reactions[1] are now broadly used to make carbon−carbon double bonds in the synthesis of pharmaceuticals, petrochemicals, fine chemicals, and polymers.[2] Catalyst design has played a crucial role in the development of synthetically useful metathesis reactions by improving catalytic performance and broadening the substrate scope. Recent research efforts have focused on highly stereoselective metathesis reactions, including *Z*-[3] or *E*-[4] selective and enantioselective metathesis.[5] Mostly, the metathesis reactions are used to construct more complex molecules by stitching two olefin fragments together. Nevertheless, cross metathesis reaction can be applied to break down large molecules into smaller parts. Cross metathesis with ethylene, known as ethenolysis,[6] has attracted much attention lately owing to the application in biomass conversion to value-added chemicals: synthesis of terminal olefins from renewable seed oil feedstocks.[7] The terminal olefins (**1** and **2** in Figure 1) are important building blocks[8] (e.g., for poly α-olefins), and the ethenolysis process can allow production of linear α-olefins from naturally occurring seed oils containing fatty acid methyl esters (FAMEs).

In the ethenolysis, catalytic activity (turnover number) and selectivity for the desired terminal alkene over the self-metathesis and secondary metathesis byproducts (**3** and **4**) are the major issues (Figure 1).[6,9,10] The use of 1,3-bis(2,4,6-trimethylphenyl)-4,5-dihydroimidazol-2-ylidene (SIMes, **G2**) and the chelating 2-isopropoxybenzylidene ligand (**HG2**) by Grubbs and co-workers[11] and Hoveyda and co-workers,[12] respectively, led to a significant increase in the activity and stability of metathesis catalysts. Highly σ-donating *N*-heterocyclic carbenes (NHC)[13] are usually the ligand of choice for ruthenium-catalyzed stereoselective olefin metathesis reactions.[1,14] It is also important to note that sterically unsymmetrical substitution patterns on NHCs turned out to

Received: July 10, 2019

DOI: 10.1021/acs.organomet.9b00469
Organometallics XXXX, XXX, XXX−XXX

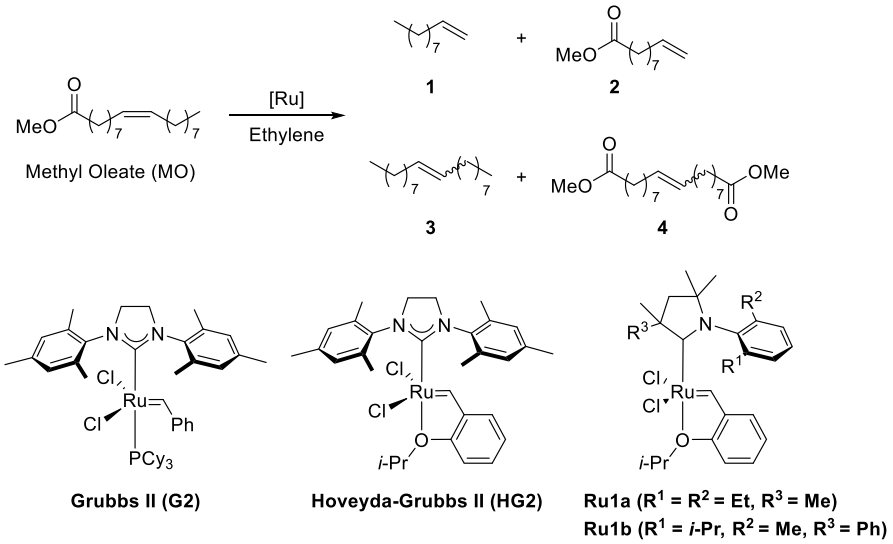

Figure 1. Ethenolysis of methyl oleate and selected ruthenium catalysts.

be important for highly α-olefin selective ethenolysis.[15] Lack of steric interaction on one side can favor a "non-productive" metathesis[16] event of the methylidene intermediates with terminal olefin products to regenerate the same methylidene intermediate, thus minimizing the formation of a different alkylidene intermediate which would lead to the formation of internal olefin byproducts. Note that the ruthenium catalyst (**Ru1**)[18] with a cyclic alkyl amino carbene (CAAC) ligand[17] which is highly σ-donating and unsymmetrically substituted, constitutes one of the current best catalysts for ethenolysis, showing up to 340 000 turnover number (TON) at low catalyst loading (1 ppm) with highly pure ethylene (99.995%).[19]

Although the steric profiles of NHC ligands can be easily modulated by substitution of *N*-aryl or -alkyl groups, lack of steric interaction on one side can induce dimerization through the Wanzlick equilibrium and undermine the stability of the complexes.[20] Imidazo[1,5-*a*]pyridin-3-ylidene carbene (ImPy), first reported in 2005 independently by J. M. Lassaletta[21] and F. Glorius,[22] has an intrinsically unsymmetrical structure with unique steric hindrance on one side[23] and is also known to be strongly σ-donating owing to the extended π-fused system.[24] Substituents (R^1) on the C5-position of ImPy can be positioned near a metal center, consequently, possibly generating a metal−substituent interaction (Figure 2). Owing to this feature, several highly sterically demanding ImPy ligands have been developed for various organometallic complexes and reactions.[23,24] However, ethenolysis reaction would require less sterically demanding ImPy ligands because the ethenolysis reaction uses sterically hindered substrates as the starting materials and high cross-metathesis selectivity is expected for unsymmetrical frameworks of ImPy ligands leaving one side relatively open (Figure 2). Thus, we envisioned that fluorine substituted ImPy ligands could be an ideal unsymmetrically substituted NHC ligand because fluorine is not sterically demanding and a possible Ru−F interaction can help to stabilize the Ru alkylidene intermediate. To the best of our knowledge, the ruthenium complexes with fluorinated ImPy ligands (F-ImPy-Ru, **Ru5** in Figure 2) have not been reported.

In the previously reported fluorine-containing NHC-ruthenium catalysts, fluorine groups can be placed at the *N*-

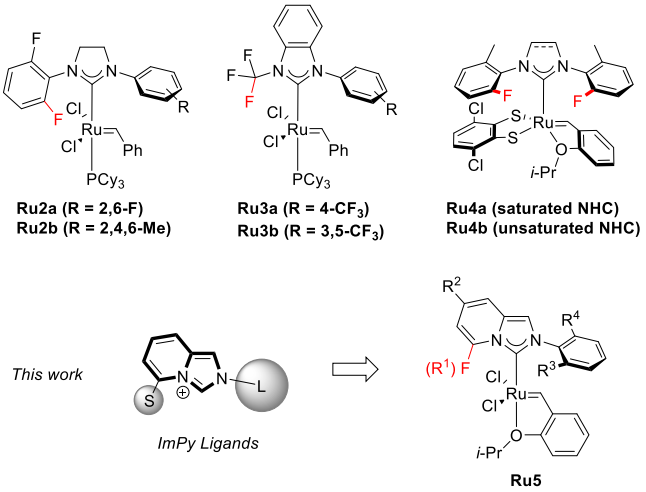

Figure 2. Fluorinated NHC-Ru complexes.

substituents on the NHC ligands (**Ru2** and **Ru3** in Figure 2).[9b,25] In those cases, Ru−F distance is expected to be short enough to consider Ru−F interaction.[9b,25e] The fluorinated aryl or alkyl groups on the ligand structures also improve the π-back-donation from the metal.[9a,26] Interestingly, these fluorinated NHC-ruthenium metathesis catalysts, which was proposed to reduce the energy barrier of phosphine dissociation by Ru−F interaction, showed enhanced activity in ring-closing metathesis[25e] and improved selectivity in alternating copolymerization and ethenolysis.[9a,b] Recently, Grubbs[4d,e] and Hoveyda[25a] independently reported that stereoretentive metathesis reaction and highly *Z*-selective metathesis of electron-deficient alkenes could be carried out by the dithiolate-ligated ruthenium complexes (**Ru4**) bearing fluorine atoms on NHCs.

Herein we describe the synthesis of highly stable ruthenium complexes bearing fluorinated unsymmetrical ImPy ligands with various substituents on both backbone and nitrogen atom of the ligands. To elucidate the electronic properties of F-ImPy ligands, a Tolman Electronic Parameters (TEP) study was conducted using iridium carbonyl carbene complexes [Ir-$(CO)_2$(ImPy)Cl]. The ^{77}Se NMR study on the selenium adducts [ImPy═Se] revealed that the π-accepting properties

DOI: 10.1021/acs.organomet.9b00469
Organometallics XXXX, XXX, XXX−XXX

of F-ImPy ligands were enhanced while holding the σ-donacity. In the selective ethenolysis of methyl oleate, *cis*-cyclooctene, and squalene, F-ImPy-Ru catalysts show high selectivity for the formation of terminal olefins and high thermal stability under an ethylene atmosphere.

RESULTS AND DISCUSSION

Synthesis of Ruthenium Catalysts. The F-ImPy-Ru complexes with various *N*-aryl groups (**Ru5a**–**Ru5e**) and variously substituted pyridine backbones (**Ru5f**–**Ru5h**) were prepared by the following procedures (Schemes 1 and 2). The

Scheme 1. Synthesis of Ruthenium Complexes (Ru5a–Ru5e)[a]

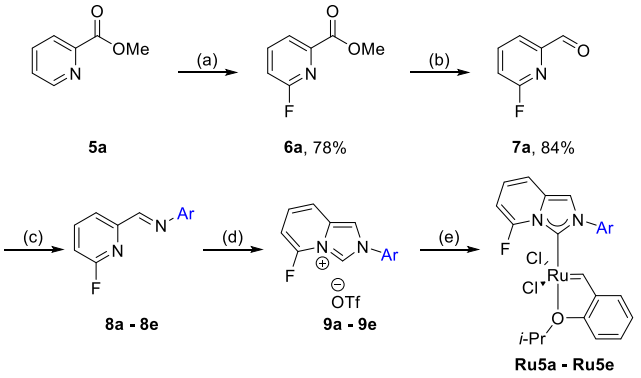

Ar =					
	i-Pr, *i*-Pr	Et, Et	Et, Me	*i*-Pr	*t*-Bu
	8a (96%)	**8b** (97%)	**8c** (95%)	**8d** (90%)	**8e** (83%)
	9a (84%)	**9b** (72%)	**9c** (51%)	**9d** (83%)	**9e** (47%)
	Ru5a (66%)	**Ru5b** (43%)	**Ru5c** (33%)	**Ru5d** (50%)	**Ru5e** (56%)

[a]Reaction conditions: (a) AgF_2, CH_3CN, rt, 1 h; (b) DIBAL-H, DCM, −55 °C, 3 h; (c) anilines, EtOH, reflux, 12 h; (d) AgOTf, $ClCH_2OPiv$, DCM, 40 °C, 12 h; (e) KHMDS, THF, **HG1**, 2 h.

fluoropyridine derivatives (**6**) were synthesized by selective fluorination with AgF_2 in CH_3CN according to a report by the Hartwig group.[27] The fluoropyridine carboxaldehydes (**7a**, **7f**, **7g**, and **7h**) were obtained by either DIBAL-H reduction of the fluorinated pyridine carboxylate (for **6a**, **6g**, and **6h**) or lithiation of 2-bromopyridine (for **6f**) followed by the reaction with DMF, in reasonable isolated yields. Then, imine formation (**8**) with anilines followed by cyclization with AgOTf and chloromethyl pivalate according to a reported procedure by the Glorius group,[22] provided the F-ImPy ligands (**9a**–**9h**) in good overall isolated yields. R^1-substituted ligands in **12**, **14**, and **16** were then synthesized by either Glorius's method[22] or by Aron's method[28] (Scheme 3). ImPy-Ru complexes were synthesized as follows: *in situ* deprotonation of imidazopyridinium salts using potassium hexamethyldisilazide (KHMDS), followed by the reaction with $RuCl_2(PCy_3)(=CH\text{-}o\text{-}O\text{-}i\text{-}PrC_6H_4)$ (**HG1**) to afford Hoveyda-type Ru complexes as brown-green solid (**Ru5a**–**Ru5h**) and as green solid (**Ru6**, **Ru7**) in reasonable isolated yields (Schemes 1, 2, and 3). These chelated benzylidene complexes are stable under ambient conditions (air and moisture). However, the stability of complex **Ru8** was much lower than that of other complexes, resulting in decomposition. The complex might be decomposed by the C–H activation pathway of the proton of the C5-

Scheme 2. Synthesis of Ruthenium Complexes (Ru5f–Ru5h)[a]

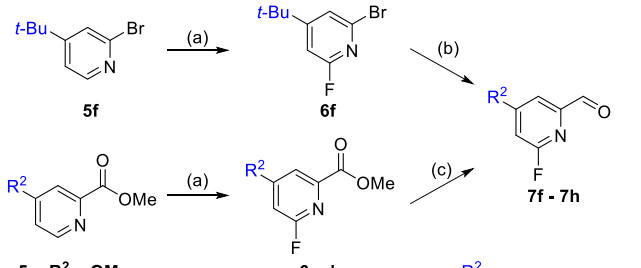

R^2	6	7	8	9	Ru5
t-Bu (**f**)	63%	84%	100%	50%	56%
OMe (**g**)	76%	76%	100%	20%	37%
Cl (**h**)	80%	76%	96%	81%	52%

[a]Reaction conditions: (a) AgF_2, CH_3CN, rt, 1 h; (b) *n*-BuLi, THF, −78 °C then DMF; (c) DIBAL-H, DCM, −55 °C, 3 h; (d) 2-*tert*-butyl aniline, EtOH, reflux, 12 h; (e) AgOTf, $ClCH_2OPiv$, DCM, 40 °C, 12 h; (f) KHMDS, THF, **HG1**, 2 h.

Scheme 3. Synthesis of Ruthenium Complexes (Ru6, 7a, b)[a]

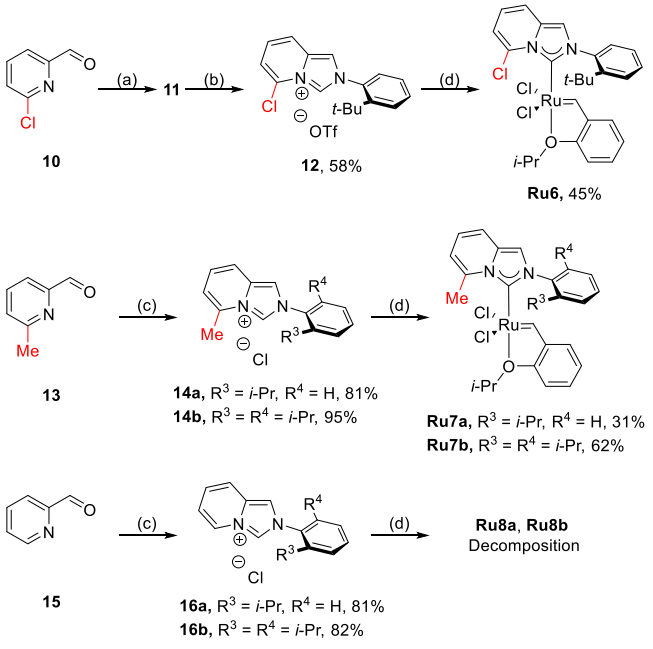

[a]Reaction conditions: (a) 2-*tert*-butyl aniline, EtOH, reflux, 12 h; (b) AgOTf, $ClCH_2OPiv$, DCM, 40 °C, 12 h; (c) anilines, formalin, HCl, EtOH, rt, 12 h, (d) KHMDS, THF, **HG1**, 2 h.

position.[29] It is important to note that substituents at the C5-position play an important role to stabilize the ruthenium complexes. The complexes were characterized by NMR, elemental analysis, high resolution mass spectrometry (HR-MS), and X-ray crystallography analysis.

X-ray Crystallographic Studies. Single crystals suitable for X-ray crystallography analysis were grown by slow diffusion of hexane through the solution of catalysts in dichloromethane

DOI: 10.1021/acs.organomet.9b00469
Organometallics XXXX, XXX, XXX–XXX

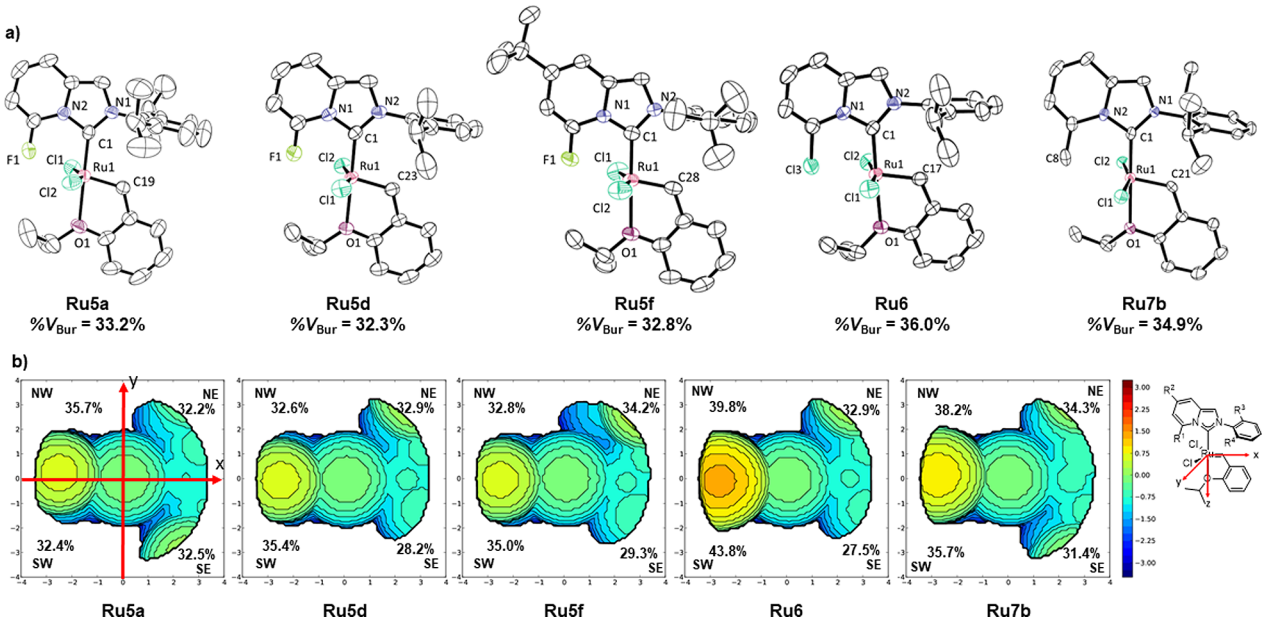

Figure 3. X-ray structures of imidazopyridine carbene−ruthenium complexes. [a]%V_{Bur} values and [b]topographic steric maps are calculated using X-ray crystallographic data.

Table 1. Selective Bond Lengths [Å] and Angles [deg] for Ru5a, Ru5d, Ru5f, Ru6, and Ru7b

Bond length [Å]	Ru5a	Ru5d	Ru5f	Ru6	Ru7b
Ru−C1$_{NHC}$	1.956(5)	1.961(2)	1.972(5)	1.967(3)	1.972(4)
Ru=C$_{carbene}$	1.822(5)	1.826(2)	1.803(5)	1.840(3)	1.831(3)
Ru−R^1	2.688(3)	2.679(2)	2.700(3)	2.7194(8)	2.925(3)
Ru−O	2.282(3)	2.258(2)	2.274(3)	2.294(2)	2.300(3)
Bond angle [deg]	**Ru5a**	**Ru5d**	**Ru5f**	**Ru6**	**Ru7b**
N−C1$_{NHC}$−N	101.8(3)	102.2(2)	102.4(4)	102.0(2)	101.4(3)
N−C1$_{NHC}$−Ru	120.8(3)	120.8(2)	120.5(3)	122.1(2)	124.3(2)
Cl−Ru−Cl	154.13(5)	160.03(3)	155.13(6)	165.43(3)	162.32(4)

at 25 °C. The % buried volume (%V_{Bur})[30] and topographic steric maps were calculated to compare steric properties of new ligands by the *SambVca 2*.[31] The solid-state structures showed that the complexes exhibit distorted square pyramidal geometries and the *N*-aryl groups are located above the *O*-chelated benzylidene (Figure 3). Although the ImPy−Ru catalysts are structurally similar to ruthenium catalysts bearing imidazolium ligands, the Ru−C$_{NHC}$ bonds (1.956(5) Å to 1.972(5) Å) in **Ru5**s are shorter than the bond (1.980(4) Å) in **HG2**[12] bearing SIMes. This result is consistent with increasing electron density at the carbene center via the π-fused system.[24c]

The R^1 substituents are constantly placed next to the ruthenium metal center. Ru−F interaction could be proposed since the Ru−F distances are shorter than 3.52 Å, the sum of the van der Waals radii of ruthenium and fluorine,[25f] as shown in Table 1 [**Ru5a** (Ru−F1 = 2.688(3) Å), **Ru5d** (Ru−F1 = 2.679(2) Å), and **Ru5f** (Ru−F1 = 2.700(3) Å)]. Chloride also could be proposed to interact with ruthenium, judged by the Ru−Cl distance in **Ru6** (Ru−Cl3 = 2.7194(8) Å). Since a methyl group is sterically larger than the fluorine atom, the Ru−C8 distance in Me−ImPy (**Ru7b**) is considerably longer (Ru−C8 = 2.925(3) Å) than those of F-ImPy (**Ru5a**, **d**, and **f**).

The topographic steric maps in Figure 3 showed the quadrantal %V_{Bur} values to consider the steric hindrance. The highly sterically demanding ligands are Cl-ImPy (**Ru6**) and Me-ImPy (**Ru7b**), and their %V_{Bur} of west side values (41.8% and 37.0%, respectively) are higher than those of F-ImPy ligands (**Ru5a**, 34.05%; **Ru5d**, 34%; **Ru5f**, 33.9%). The variation of *N*-aryl groups (2,6-diisopropylphenyl (DIPP) in **Ru5a**, 2-isopropylphenyl (IPP) in **Ru5d**, and 2-*tert*-butylphenyl (TBP) in **Ru5f**) significantly influences the %V_{Bur} of the southeast side (**Ru5a**, 32.5%; **Ru5d**, 28.2%; **Ru5f**, 29.3%). The %V_{Bur} values have a correlation with activity and selectivity, which will be discussed later.

Electronic Properties of ImPy Ligands by IR and NMR. The Tolman electronic parameter (TEP) is the most widely used method to evaluate the electronic properties of the ligands.[32] The carbonyl vibrations of iridium carbonyl complexes bearing NHC ligands are measured by FT-IR spectroscopy. Iridium complexes [Ir(CO)$_2$(ImPy)Cl] were synthesized by the reactions between R^1-substituted ImPy ligands (F-, Cl-, and Me-) and [Ir(COD)Cl]$_2$ and were subsequently treated with carbon monoxide at room temperature in CH_2Cl_2 (Scheme 4). The TEP values were calculated from the average CO stretching vibration obtained in CH_2Cl_2 solution (Table 2). It is interesting to note that the TEP values of [Ir(CO)$_2$(R^1-ImPy)Cl] complexes are between 2049 and 2053 cm^{-1}, which are slightly stronger than those of the original ImPy ligands (2053 to 2057 cm^{-1}).[21,24a] We expected higher TEP values because of the electron-withdrawing substituents on the ImPy ligands. Although TEP parameters

DOI: 10.1021/acs.organomet.9b00469
Organometallics XXXX, XXX, XXX−XXX

Scheme 4. Synthesis of $[Ir(CO)_2(R^1\text{-ImPy})Cl]$[a]

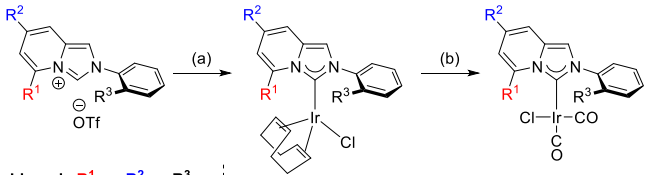

Ligand	R^1	R^2	R^3		Quantitative Yield
9e	F	H	*t*-Bu	**Ir1**, 69%	**Ir6**
9f	F	*t*-Bu	*t*-Bu	**Ir2**, 65%	**Ir7**
9h	F	Cl	*t*-Bu	**Ir3**, 62%	**Ir8**
12	Cl	H	*t*-Bu	**Ir4**, 85%	**Ir9**
16a	Me	H	*i*-Pr	**Ir5**, 60%	**Ir10**

[a]Reaction conditions: (a) KHMDS, THF, $[Ir(COD)Cl]_2$; (b) CO (1 atm), CH_2Cl_2, rt.

Table 2. Tolman Electronic Parameters (TEP) and ^{77}Se NMR Shifts of Selected ImPy

entry	L	(R^1, R^2, R^3)	[Ir] $\nu_{av(CO)}$[a] [cm^{-1}]	[Ir] TEP[a] [cm^{-1}]	^{77}Se[b] δ [ppm]
1	**9e**	(F, H, *t*-Bu)	2024	2051	175.92
2	**9f**	(F, *t*-Bu, *t*-Bu)	2023	2051	166.74
3	**9h**	(F, Cl, *t*-Bu)	2025	2053	192.04
4	**12**	(Cl, H, *t*-Bu)	2021	2049	210.72
5	**14a**	(Me, H, *i*-Pr)	2022	2050	154.75

[a]The IR spectra of complexes were measured in CH_2Cl_2, and TEP values were calculated from the symmetric and antisymmetric CO stretching frequencies of the corresponding $[Ir(CO)_2(ImPy)Cl]$ complexes, using the equation TEP = 0.8475 × $\nu_{av(CO)}$ + 336.2 cm^{-1}. [b]^{77}Se-NMR spectra in $CDCl_3$.

indicate the combined properties of σ-donor and π-acceptor, R^1-substituted ImPy ligands turn out to be as electron-donating as the original ImPy.

To further investigate the π-accepting ability of the ligands, ^{77}Se NMR studies were conducted on [ImPy=Se] adducts (Scheme 5, Table 2).[33] Interestingly, the ^{77}Se-NMR chemical

Scheme 5. Synthesis of [ImPy=Se][a]

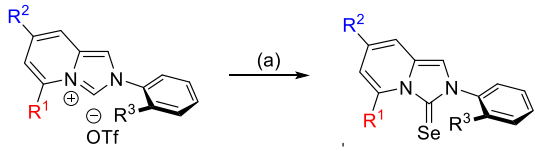

Ligand	R^1	R^2	R^3	
9e	F	H	*t*-Bu	**Se1**, 72%
9f	F	*t*-Bu	*t*-Bu	**Se2**, 76%
9h	F	Cl	*t*-Bu	**Se3**, 32%
12	Cl	H	*t*-Bu	**Se4**, 73%
14a	Me	H	*i*-Pr	**Se5**, 76%
16a	H	H	*i*-Pr	**Se6**, 39%

[a]Reaction conditions: (a) KHMDS, THF, Se.

shifts (entries 1–4) of the F-ImPy and Cl-ImPy appeared downfield (175 to 210 ppm). This observation shows that the electronegative halide substituents increased the π-accepting ability of the ImPy. Me-ImPy (**Se5**, entry 5) reveals unexpectedly good π-accepting character for unclear reasons. Table 2 shows that R^1-substituted ImPy ligands are more π-accepting than the unsubstituted ImPy as their ^{77}Se-NMR values are more downfield shifted compared to −12 ppm of **Se6** and those[24a] of the unsubstituted ImPy (−10 to 20 ppm). Thus, substituents at C5 of ImPy ligands seem to increase the π-accepting character without significantly lowering the σ-donating ability.

Computational Study. To theoretically study the electronic structure of ImPy ligands and rationalize the preceding experimental observations, the molecular orbitals of the R^1-ImPy ligands (**9**, **12**, and **14**) were calculated by density functional theory (DFT). Calculation of unsubstituted H-ImPy ligands (**16′**) reported in 2017 by F. Shibahara and T. Murai showed that substituents on the C1-position of imidazopyridine lowered the energy levels of the lowest unoccupied molecular orbitals (LUMOs).[24a] The R^1-ImPy ligands were calculated and the geometries of these free carbenes in their ground state were optimized at the B3LYP/6-31G(d,p) level. The methyl group was used instead of *N*-aryl groups for simplicity.

Figure 4 shows the HOMOs and LUMOs of free carbene structures in the substituted ImPy's. HOMO−1s and HOMOs act as σ-orbital of carbene carbon and π-donor orbitals, respectively, and LUMO+1s and LUMOs act as π-accepting orbitals for ImPy (**9′**, **12′**, **14′**, and **16′**). Fluorine and chlorine lower HOMOs and LUMOs, and methyl group increases those levels. This result is consistent with the fact that ImPy is a strong donor ligand. The electron density at the carbene center of ImPy's increased probably because of the π-fused system. However, energy levels are not considerably changed by the electronegative atom and electron-donating group and not significantly correlated with TEP and ^{77}Se-NMR spectral results.

Ethenolysis of Methyl Oleate. The catalytic performance of prepared F-ImPy-Ru complexes was evaluated in the ethenolysis of methyl oleate (**MO**) (Scheme 6, Table 3). The results of 86% selectivity, for terminal alkene products (**1** and **2**) over self- and secondary-metathesis products (**3** and **4**) with **Ru5a** (entry 1) showed that structurally unsymmetrical features of ImPy ligand resulted in high α-olefin selectivity, compared to the lower selectivity (33%)[9d] shown by other Hoveyda−Grubbs Ru catalysts bearing symmetrical SIMes (**HG2**). To investigate the steric effects of ImPy ligands, a range of F-ImPy-Ru complexes (**Ru5b−5e**) were tested for ethenolysis of methyl oleate using 100 ppm catalyst and 150 psi of ethylene at 60 °C. The complexes **Ru5b** and **Ru5c** exhibited higher conversion (20% and 14%) and turnover number (TON, 1500 and 1000) than **Ru5a** (5% and 550 TON) but lower selectivity presumably due to the decreased steric hindrance on the east side *N*-aryl groups (entries 2 and 3). The use of a mono-*ortho*-substituted *N*-aryl group (**Ru5d** and **Ru5e**) enhanced the TONs to 2200 and 3400 while maintaining high selectivity of 82% and 79% (entries 4 and 5). As long as it is a monosubstituted aryl (R^4 = H), a bulkier *ortho* substituent seems to be better for overall catalyst efficiency (R^3 = *t*-Bu for **Ru5e** vs *i*-Pr for **Ru5d**). According to the steric map of $\%V_{Bur}$ (Figure 3b), the southeast side $\%V_{Bur}$ of **Ru5d** is slightly diminished (28.2%) compared to that of **Ru5a** (32.5%). Modulation of steric bulk of the east side resulted in higher selectivity in ethenolysis.

Table 4 summarizes the effects of backbone substitution of F-ImPy-Ru catalysts. Complex **Ru5f** containing a σ-donating *t*-Bu group on the backbone enhances catalytic activity with 51% conversion and TON of 3900, compared to complex **Ru5e** (entry 1 vs entry 5 in Table 3). However, catalysts **Ru5g** and **Ru5h** provided lower conversions compared to **Ru5e** (entries 2 and 3 vs entry 5 in Table 3). π-Donating groups in complexes **Ru5g** and **Ru5h** seem ineffective as they exhibit

DOI: 10.1021/acs.organomet.9b00469
Organometallics XXXX, XXX, XXX−XXX

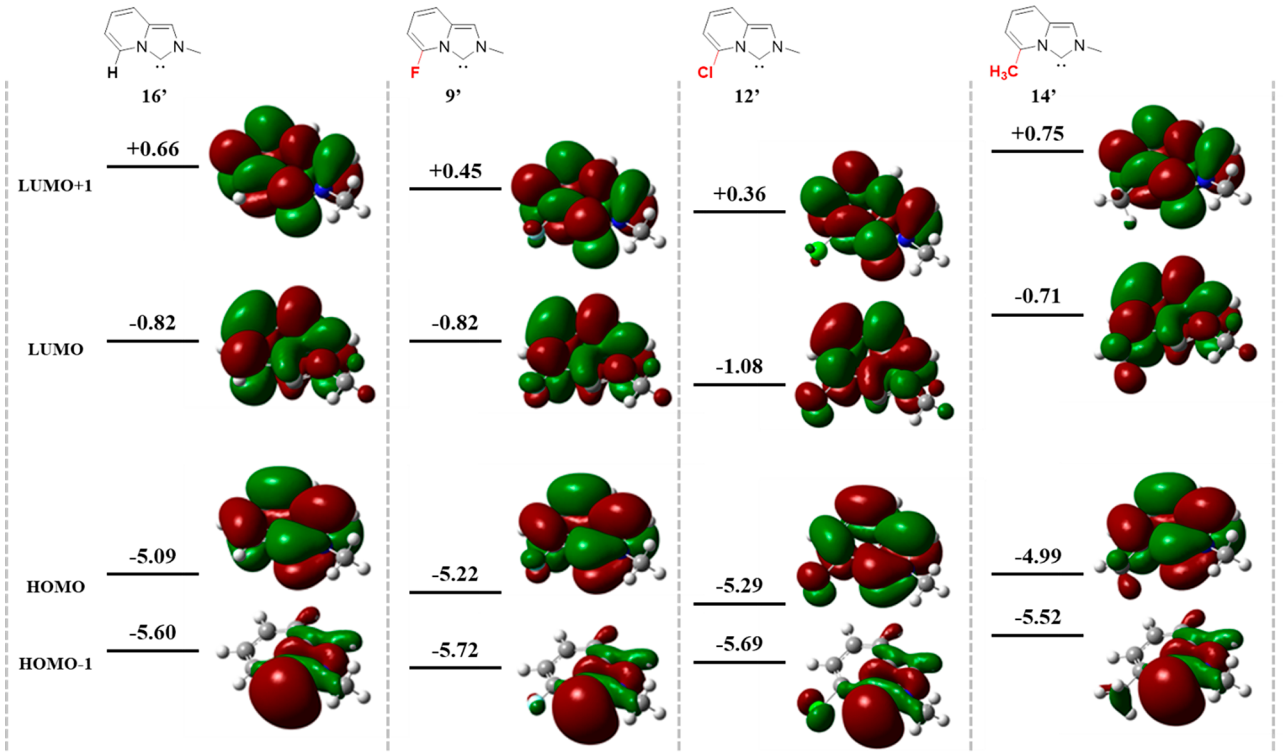

Figure 4. HOMO and LUMO energy levels (eV) of free carbenes of ImPy ligand, F-ImPy (**9′**), Cl-ImPy (**12′**), Me-ImPy (**14′**) and H-ImPy (**16′**) at the B3LYP/6-31G(d,p) level.

Scheme 6. Ethenolysis of Methyl Oleate with F-ImPy-Ru Complexes

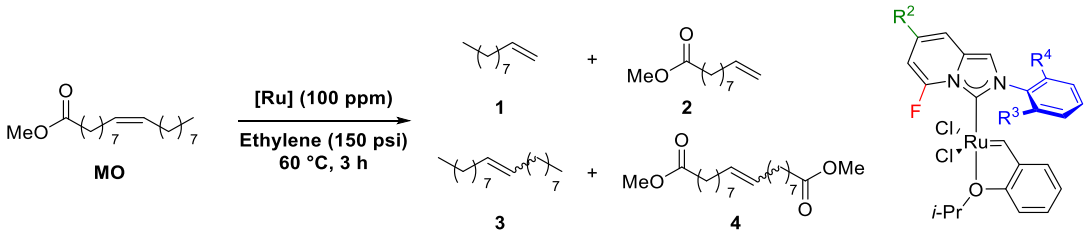

Table 3. Ethenolysis with Catalysts Bearing Sterically Different Aryl Substituents (Ru5a–5e)[a]

entry	cat	R^3	R^4	conv. (%)[b]	selectivity (%)[c]	yield (%)[d]	TON[e]
1	**Ru5a**	*i*-Pr	*i*-Pr	6	86	5	550
2	**Ru5b**	Et	Et	20	78	15	1500
3	**Ru5c**	Et	Me	14	74	10	1000
4	**Ru5d**	*i*-Pr	H	26	82	22	2200
5	**Ru5e**	*t*-Bu	H	44	79	34	3400

[a]Reaction conditions: catalyst (100 ppm), C_2H_4 (150 psi, 99.95% purity), 60 °C, 3 h; Conversion, selectivity were determined by GC using tridecane as an internal standard. [b]Conversion = 100 − [(final moles **MO**) × 100/(initial moles **MO**)]. [c]Selectivity = 100 × (moles **1** + **2**)/[(moles **1** + **2**) + (2 × moles of **3** + **4**)]. [d]Yield = Conversion × Selectivity/100. [e]TON = Yield × (initial moles **MO**/moles catalyst)/100.

Table 4. Ethenolysis with Catalysts Bearing Electronic and Steric Substituents on ImPy (9f–9h, 12, and 14)[a]

entry	cat.	R^1	R^2	conv. (%)[b]	selectivity (%)[c]	yield (%)[d]	TON[e]
1	**Ru5f**	F	*t*-Bu	51	77	39	3900
2	**Ru5g**	F	OMe	34	81	27	2700
3	**Ru5h**	F	Cl	27	83	23	2300
4	**Ru6**	Cl	H	<1			
5	**Ru7a**	Me	H	7	91	6	600

[a]Reaction conditions: catalyst (100 ppm), C_2H_4 (150 psi, 99.95% purity), 60 °C, 3 h; Conversion, selectivity were determined by GC using tridecane as an internal standard. [b]Conversion = 100 − [(final moles **MO**) × 100/(initial moles **MO**)]. [c]Selectivity = 100 × (moles **1** + **2**)/[(moles **1** + **2**) + (2 × moles of **3** + **4**)]. [d]Yield = Conversion × Selectivity/100. [e]TON = Yield × (initial moles **MO**/moles catalyst)/100.

lower TONs. As a control experiment probing the fluorine atom effect, the Cl-ImPy ruthenium complex (**Ru6**) was prepared (Scheme 3) and tested for ethenolysis, but the **Ru6** did not show catalytic activity (entry 4). The chlorinated ImPy is highly sterically demanding as chlorine atom is coordinated to the metal, and $\%V_{Bur}$ of the west side of **Ru6** in Figure 3 is 41.8%, which is higher than that of other F-ImPy-Ru (**Ru5d**, 34.0%). High selectivity of 91% was obtained with Me-ImPy-Ru (**Ru7**), but TON was lower presumably because of the increased steric hindrance of the methyl group (entry 5). The $\%V_{Bur}$ of the west side of **Ru7** in Figure 3 is 37.0%, which is

DOI: 10.1021/acs.organomet.9b00469
Organometallics XXXX, XXX, XXX−XXX

Table 5. Different Catalysts Loadings, Temperature, and Ethylene Pressure Effects on Ethenolysis[a]

entry	cat.	loading (ppm)	temp. (°C)	pressure (psi)	conversion (%)[b]	selectivity (%)[c]	yield (%)[d]	TON[e]
1	**Ru5f**	50	60	150	32	77	25	5100
2	**Ru5f**	20	60	150	19	71	13	6700
3	**Ru5f**	200	60	150	68	79	54	2700
4	**Ru5f**	500	60	150	69	84	58	1200
5	**Ru5f**	200	60	300	62	83	52	2600
6[f]	**Ru5f**	100	40	150	25	77	19	1900
7	**Ru5f**	100	80	150	55	76	42	4200
8	**Ru5f**	100	100	150	57	72	40	4000
9	**Ru5f**	500	80	150	74	82	60	1200
10[g]	**Ru1a**	50	50	200	89	76	67	13500
11[h]	**Ru1a**	500	50	150	86	82	70	1400
12[i]	**Ru5f**	500	60	150	55	82	45	900
13[i]	**Ru5f**	100	60	150	14	84	12	1200

[a]Reaction conditions: catalyst (ppm), temperature (°C), C_2H_4 (psi, 99.95% purity), 3 h; Conversion, selectivity were determined by GC using tridecane as an internal standard. [b]Conversion = 100 − [(final moles **MO**) × 100/[initial moles **MO**)]. [c]Selectivity = 100 × (moles **1** + **2**)/[(moles **1** + **2**) + (2 × moles of **3** + **4**)]. [d]Yield = Conversion × Selectivity/100. [e]TON = Yield × (initial moles **MO**/moles catalyst)/100. [f]Reaction for 12 h. [g]Reference 15a. [h]Reference 15c. [i]Reaction with MO (96%).

Table 6. Ethenolysis of *cis*-Cyclooctene[a]

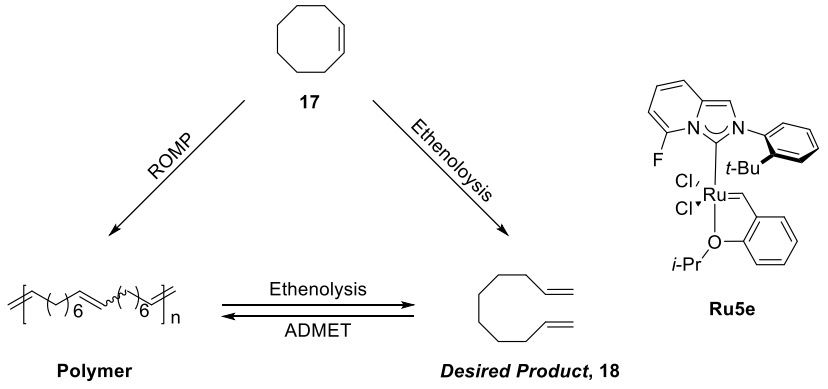

entry	loading (ppm)	pressure (psi)	conv. (%)[b]	selectivity (%)[c]	yield (%)[d]
1	**100**	150	70	22	15
2	**200**	150	69	25	17
3	**500**	150	70	48	33
4	**1000**	150	73	47	34
5[e]	**500**	150	91	15	14
6	**500**	200	68	48	33
7	**500**	300	60	56	34

[a]Reaction conditions: catalyst (ppm), temperature (60 °C), C_2H_4 (psi, 99.95% purity), 5 h; Conversion, selectivity were determined by GC using tridecane as an internal standard. [b]Conversion = 100 × (1 − final moles **17**/initial moles **17**). [c]Selectivity = 100 × (final moles **18**)/(initial moles **17** − final moles **17**). [d]Yield = 100 × final moles **18**/initial moles **17**. [e]Reaction at 100 °C.

higher than other F-ImPy-Ru (**Ru5a**, 34.05%; **Ru5d**, 34%; **Ru5f**, 33.9%).

Table 5 summarizes further optimization of reaction conditions in terms of catalyst loading, reaction temperature, and ethylene pressure. Lowering the catalyst loading to 20 ppm showed a slight loss of the selectivity but was still efficient in ethenolysis reaction (entry 2). Raising the catalyst loading to 200 and 500 ppm led to the improved yield (54% and 58%) and selectivity (79% and 84%, entries 3 and 4). Note that the selectivity data shown by **Ru5f** (entries 1 and 4) are similar to those shown by the CAAC-Ru catalyst **Ru1a**[15a,c] (entries 10 and 11). At 60 °C, **Ru5f** showed the selectivity of 77% (50 ppm, entry 1) and 84% (500 ppm, entry 4), and unsymmetrical CAAC-Ru catalyst **Ru1a** showed 76% (50 ppm, entry 10)[15a] and 82% (500 ppm, entry 11)[15c] at 50 °C. These results indicate that the structurally unsymmetrical feature of ImPy ligand gave high selectivity as the structurally related **Ru1a** catalysts (bearing unsymmetrical CAAC) showed similarly high selectivity under similar conditions. At high pressure (300 psi), the selectivity (83%) increased due to the increased ethylene solubility in methyl oleate (entry 5). Ethenolysis reactions were conducted at 40, 60, 80, and 100 °C with catalyst **Ru5f**. Notably, similar TON and slightly lower selectivity were obtained at high temperatures, even at 100 °C (entries 7 and 8). The conversion of 74%, the selectivity of 82% and yield of 60% were obtained with 500 ppm catalyst at 80 °C (entry 9) whereas similar conversion of 69% and slightly increased selectivity of 76% and yield of 42% were obtained with 500 ppm catalyst at 60 °C (entry 4). We also examined the influence of methyl oleate purity (96%). Recently, Grela

DOI: 10.1021/acs.organomet.9b00469
Organometallics XXXX, XXX, XXX−XXX

Scheme 7. Ethenolysis of Squalene with F-ImPy-Ru Complex

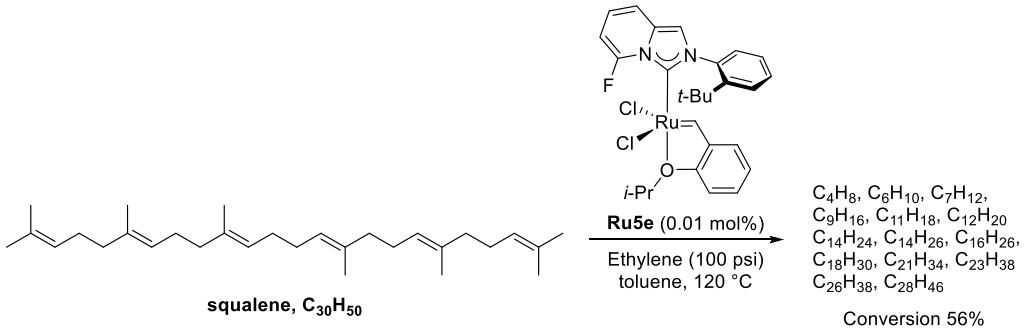

and co-workers reported that the robust ruthenium catalysts bearing unsymmetrical NHCs could be operative with less pure reagents under the practical conditions.[15b] At 500 ppm catalyst loading, **Ru5f** catalyst was still efficient in ethenolysis reaction when the less pure methyl oleate (96% purity) was used after filtering through activated alumina (entry 12). However, with 100 ppm of **Ru5f**, the conversion is significantly reduced, while ruthenium catalysts bearing unsymmetrical NHCs reported in the literature[15b] still showed remarkable efficiencies with less pure reagents. Only a few ruthenium catalysts showed high thermal stability under an ethylene atmosphere at high temperature.[15c,34] Typically, activity and selectivity were reduced, and also the isomerization products were obtained owing to the decomposed, ruthenium hydride species.[35] Interestingly, the current results suggest the formation of highly stable ruthenium intermediate at high reaction temperatures without catalyst decomposition. It is worth noting that the development of the thermally robust catalysts under ethylene is important for the ethenolysis of tri- or tetrasubstituted olefins.[6a]

Ethenolysis of *cis*-Cyclooctene. The cyclic alkenes are challenging substrates because of the highly competitive ring-opening metathesis polymerization reaction (ROMP). Recently, ethenolysis of *cis*-cyclooctene was carried out by Ru-based catalysts (Togni and co-workers)[9a] and Mo-based catalysts (Schrock, Hoveyda, and co-workers).[10b] The ethenolysis of methyl oleate results with F-ImPy-Ru catalysts led us to investigate the ethenolysis of *cis*-cyclooctene using the catalyst **Ru5e** (Table 6). Table 6 summarizes optimization of reaction conditions in terms of catalyst loading, temperature, and ethylene pressure. **Ru5e** bearing a structurally unsymmetrical ImPy ligand slightly improved selectivity (22%), compared to the lower selectivity (12%) shown by Grubbs Ru catalysts bearing symmetrical NHCs (**G2**).[9a] Raising the catalyst loading to 500 ppm led to the improved yield (17% to 33%) and selectivity (25% to 48%, entry 2 and 3). Analogously, the ethenolysis conversion of 73%, the selectivity of 47%, and a yield of 34% were obtained with 1000 ppm catalyst loading (entry 4). Unfortunately, the increased temperature led to mainly ROMP and secondary metathesis products (entry 5). Although the selectivity of **18** decreased, the activity of **Ru5e** was still efficient at 100 °C. This result is consistent with highly thermally stable **Ru5f** under the ethenolysis conditions. At high pressure (200 and 300 psi), the selectivity was retained or increased but conversion was reduced (entries 5 and 6) probably because of the decomposed catalysts. It turns out that 500 ppm catalyst loading, 60 °C, and 150 psi gave the optimal catalytic performance (70% conversions, 47% selectivity, and 33% yield). The results also show that **Ru5e** is useful for another type of ethenolysis.

Ethenolysis of Squalene. We expected that the thermally stable F-ImPy-Ru catalysts could be efficient in ethenolysis of trisubstituted olefins, which typically requires high reaction temperature (Scheme 7). Previously, the Plenio group demonstrated the ethenolysis of squalene (containing six trisubstituted olefins), natural rubbers,[34a] and end-of-life tire.[34b] **Ru5e** catalyst (100 ppm per double bond) was tested in the ethenolysis of squalene at 120 °C with 100 psi ethylene pressure. To our delight, the F-ImPy-Ru catalyst **Ru5e** gave 56% conversion. It is worth noting that highly selective and thermally robust catalysts under ethylene can be effective for the ethenolysis of trisubstituted olefins.

■ CONCLUSION

Herein we report the synthesis of novel ruthenium catalysts with unsymmetrical F-ImPy ligands and their application in catalytic ethenolysis of methyl oleate, *cis*-cyclooctene, and squalene containing trisubstituted olefins. Effects of ligand structure variations on catalyst activity, selectivity, and thermal stability were studied. Ru−F interaction has been identified in the solid state from X-ray analysis, and the F−Ru interaction might help to stabilize the ruthenium complexes. F-ImPy-Ru catalyst **Ru5f** with an *ortho-tert*-butyl-phenyl substituent on nitrogen and a σ-donating *t*-Bu group on the pyridine backbone resulted in high TON (up to 6700) and high selectivity (up to 86%) for the formation of terminal olefins in ethenolysis of methyl oleate. F-ImPy-Ru catalyst **Ru5f** was stable at high temperature, even 100 °C. We also observed that the F-ImPy-Ru catalyst **Ru5e** is effective in more challenging ethenolysis reactions, giving 70% conversions, 48% selectivity, and 33% yield for the ethenolysis of *cis*-cyclooctene at 60 °C, and 56% conversion for the ethenolysis of squalene at 120 °C. Currently, further development of more reactive catalysts is in progress in our laboratory.

■ ASSOCIATED CONTENT

Supporting Information

The Supporting Information is available free of charge on the ACS Publications website at DOI: 10.1021/acs.organomet.9b00469.

Detailed synthetic procedures, analytical data, and X-ray crystallographic data for new compounds (PDF)

Accession Codes

CCDC 1587184−1587188 contain the supplementary crystallographic data for this paper. These data can be obtained free of charge via www.ccdc.cam.ac.uk/data_request/cif, or by

DOI: 10.1021/acs.organomet.9b00469
Organometallics XXXX, XXX, XXX−XXX

emailing data_request@ccdc.cam.ac.uk, or by contacting The Cambridge Crystallographic Data Centre, 12 Union Road, Cambridge CB2 1EZ, UK; fax: +44 1223 336033.

AUTHOR INFORMATION

Corresponding Authors

*E-mail: wjchung@gist.ac.kr.
*E-mail: shong@gist.ac.kr.

ORCID

Ji Yeon Ryu: 0000-0001-6321-5576
Junseong Lee: 0000-0002-5004-7865
Won-jin Chung: 0000-0003-3050-4798
Sukwon Hong: 0000-0002-2078-9630

Notes

The authors declare no competing financial interest.

ACKNOWLEDGMENTS

This research was supported by the Samsung Research Funding Center of Samsung Electronics under Project Number SRFC-MA1502-11. This work was also supported by the Technology Development Program to Solve Climate Changes through the National Research Foundation (NRF) funded by the Ministry of Science, ICT & Future Planning (NRF2017M1A2A2049102), and "Nobel Research Project" grant for Grubbs Center for Polymers and Catalysis funded by the GIST in 2019.

REFERENCES

(1) (a) *Handbook of Metathesis: Grubbs/Handbook of Metathesis, Set*; Grubbs, R. H., Wenzel, A. G., O'Leary, D. J., Khosravi, E., Eds.; WileyVCH: Weinheim, Germany, 2015. (b) *Olefin Metathesis: Theory and Practice*; Grela, K., Ed.; Wiley: Hoboken, NJ, 2014. (c) Boeda, F.; Clavier, H.; Nolan, S. P. Ruthenium-Indenylidene Complexes: Powerful Tools for Metathesis Transformations. *Chem. Commun.* **2008**, 2726−2740. (d) Hoveyda, A. H.; Zhugralin, A. R. The Remarkable Metal-Catalysed Olefin Metathesis Reaction. *Nature* **2007**, *450*, 243−251. (e) Schrock, R. R.; Hoveyda, A. H. Molybdenum and Tungsten Imido Alkylidene Complexes as Efficient Olefin-Metathesis Catalysts. *Angew. Chem., Int. Ed.* **2003**, *42*, 4592−4633. (f) Connon, S. J.; Blechert, S. Recent Developments in Olefin Cross-Metathesis. *Angew. Chem., Int. Ed.* **2003**, *42*, 1900−1923. (g) Fürstner, A. Olefin Metathesis and Beyond. *Angew. Chem., Int. Ed.* **2000**, *39*, 3012−3043.

(2) For recent reviews see: (a) Haque, T.; Nomura, K. ADMET Polymerization: Greener Method for Synthesis of End-Functionalized Poly(Arylene Vinylene)S. *Green Sustainable Chem.* **2017**, *7*, 1−19. (b) Balla, Á.; Al-Hashimi, M.; Hlil, A.; Bazzi, H. S.; Tuba, R. Ruthenium-Catalyzed Metathesis of Conjugated Polyenes. *ChemCatChem* **2016**, *8*, 2865−2875. (c) Higman, C. S.; Lummiss, J. A. M.; Fogg, D. E. Olefin Metathesis at the Dawn of Implementation in Pharmaceutical and Specialty-Chemicals Manufacturing. *Angew. Chem., Int. Ed.* **2016**, *55*, 3552−3565. (d) Bachler, P. R.; Wagener, K. B. Functional Precision Polymers via ADMET Polymerization. *Monatsh. Chem.* **2015**, *146*, 1053−1061. (e) *Metathesis in Natural Product Synthesis*; Cossy, J., Arseniyadis, S., Meyer, C., Eds.; Wiley-VCH: Weinheim, Germany, 2010. (f) Bielawski, C. W.; Grubbs, R. H. Living Ring-Opening Metathesis Polymerization. *Prog. Polym. Sci.* **2007**, *32*, 1−29. (g) Nicolaou, K. C.; Bulger, P. G.; Sarlah, D. Metathesis Reactions in Total Synthesis. *Angew. Chem., Int. Ed.* **2005**, *44*, 4490−4527. (h) *Metathesis Polymerization*; Buchmeiser, M. R., Ed.; Springer: Berlin, Heidelberg, 2005.

(3) (a) Koh, M. J.; Nguyen, T. T.; Lam, J. K.; Torker, S.; Hyvl, J.; Schrock, R. R.; Hoveyda, A. H. Molybdenum Chloride Catalysts for *Z*-Selective Olefin Metathesis Reactions. *Nature* **2017**, *542*, 80−85. (b) Koh, M. J.; Nguyen, T. T.; Zhang, H.; Schrock, R. R.; Hoveyda, A. H. Direct Synthesis of *Z*-Alkenyl Halides through Catalytic Cross-Metathesis. *Nature* **2016**, *531*, 459−465. (c) Koh, M. J.; Khan, R. K. M.; Torker, S.; Yu, M.; Mikus, M. S.; Hoveyda, A. H. High-Value Alcohols and Higher-Oxidation-State Compounds by Catalytic *Z*-Selective Cross-Metathesis. *Nature* **2015**, *517*, 181−186. (d) Herbert, M. B.; Grubbs, R. H. *Z*-Selective Cross Metathesis with Ruthenium Catalysts: Synthetic Applications and Mechanistic Implications. *Angew. Chem., Int. Ed.* **2015**, *54*, 5018−5024. (e) Fürstner, A. Teaching Metathesis "Simple" Stereochemistry. *Science* **2013**, *341*, 1229713. (f) Occhipinti, G.; Hansen, F. R.; Törnroos, K. W.; Jensen, V. R. Simple and Highly *Z*-Selective Ruthenium-Based Olefin Metathesis Catalyst. *J. Am. Chem. Soc.* **2013**, *135*, 3331−3334. (g) Rosebrugh, L. E.; Herbert, M. B.; Marx, V. M.; Keitz, B. K.; Grubbs, R. H. Highly Active Ruthenium Metathesis Catalysts Exhibiting Unprecedented Activity and *Z*-Selectivity. *J. Am. Chem. Soc.* **2013**, *135*, 1276−1279. (h) Keitz, B. K.; Endo, K.; Patel, P. R.; Herbert, M. B.; Grubbs, R. H. Chelated Ruthenium Catalysts for *Z* -Selective Olefin Metathesis. *J. Am. Chem. Soc.* **2012**, *134*, 693−699. (i) Endo, K.; Grubbs, R. H. Chelated Ruthenium Catalysts for *Z*-Selective Olefin Metathesis. *J. Am. Chem. Soc.* **2011**, *133*, 8525−8527. (j) Meek, S. J.; O'Brien, R. V.; Llaveria, J.; Schrock, R. R.; Hoveyda, A. H. Catalytic *Z*-Selective Olefin Cross-Metathesis for Natural Product Synthesis. *Nature* **2011**, *471*, 461−466. (k) Hoveyda, A. H.; Ibrahem, I.; Yu, M.; Schrock, R. R. Highly *Z*- and Enantioselective Ring-Opening/Cross-Metathesis Reactions Catalyzed by Stereogenic-at-Mo Adamantylimido Complexes. *J. Am. Chem. Soc.* **2009**, *131*, 3844−3845.

(4) (a) Montgomery, T. P.; Ahmed, T. S.; Grubbs, R. H. Stereoretentive Olefin Metathesis: An Avenue to Kinetic Selectivity. *Angew. Chem., Int. Ed.* **2017**, *56*, 11024−11036. (b) Xu, C.; Liu, Z.; Torker, S.; Shen, X.; Xu, D.; Hoveyda, A. H. Synthesis of *Z*- or *E*-Trisubstituted Allylic Alcohols and Ethers by Kinetically Controlled Cross-Metathesis with a Ru Catechothiolate Complex. *J. Am. Chem. Soc.* **2017**, *139*, 15640−15643. (c) Shen, X.; Nguyen, T. T.; Koh, M. J.; Xu, D.; Speed, A. W. H.; Schrock, R. R.; Hoveyda, A. H. Kinetically *E*-Selective Macrocyclic Ring-Closing Metathesis. *Nature* **2017**, *541*, 380−385. (d) Ahmed, T. S.; Grubbs, R. H. Fast-Initiating, Ruthenium-Based Catalysts for Improved Activity in Highly *E*-Selective Cross Metathesis. *J. Am. Chem. Soc.* **2017**, *139*, 1532−1537. (e) Johns, A. M.; Ahmed, T. S.; Jackson, B. W.; Grubbs, R. H.; Pederson, R. L. High Trans Kinetic Selectivity in Ruthenium-Based Olefin Cross-Metathesis through Stereoretention. *Org. Lett.* **2016**, *18*, 772−775. (f) Nguyen, T. T.; Koh, M. J.; Shen, X.; Romiti, F.; Schrock, R. R.; Hoveyda, A. H. Kinetically controlled *E*-selective catalytic olefin metathesis. *Science* **2016**, *352*, 569−575.

(5) (a) Hoveyda, A. H. Evolution of Catalytic Stereoselective Olefin Metathesis: From Ancillary Transformation to Purveyor of Stereochemical Identity Scheme 1. Early Complexes Developed for Catalyzing Olefin Metathesis Reactions. *J. Org. Chem.* **2014**, *79*, 4763−4792. (b) Kress, S.; Blechert, S. Asymmetric Catalysts for Stereocontrolled Olefin Metathesis Reactions. *Chem. Soc. Rev.* **2012**, *41*, 4389−4408. (c) Hoveyda, A. H.; Malcolmson, S. J.; Meek, S. J.; Zhugralin, A. R. Catalytic Enantioselective Olefin Metathesis in Natural Product Synthesis. Chiral Metal-Based Complexes That Deliver High Enantioselectivity and More. *Angew. Chem., Int. Ed.* **2010**, *49*, 34−44. (d) Malcolmson, S. J.; Meek, S. J.; Sattely, E. S.; Schrock, R. R.; Hoveyda, A. H. Highly Efficient Molybdenum-Based Catalysts for Enantioselective Alkene Metathesis. *Nature* **2008**, *456*, 933−937.

(6) (a) Spekreijse, J.; Sanders, J. P. M.; Bitter, J. H.; Scott, E. L. The Future of Ethenolysis in Biobased Chemistry. *ChemSusChem* **2017**, *10*, 470−482. (b) Pfister, K. F.; Baader, S.; Baader, M.; Berndt, S.; Goossen, L. J. Biofuel by Isomerizing Metathesis of Rapeseed Oil Esters with (Bio)Ethylene for Use in Contemporary Diesel Engines. *Sci. Adv.* **2017**, *3*, No. e1602624. (c) Bidange, J.; Fischmeister, C.; Bruneau, C. Ethenolysis: A Green Catalytic Tool to Cleave Carbon−Carbon Double Bonds. *Chem. - Eur. J.* **2016**, *22*, 12226−12244. (d) Nickel, A.; Ung, T.; Mkrtumyan, G.; Uy, J.; Lee, C. W.; Stoianova, D.; Papazian, J.; Wei, W. H.; Mallari, A.; Schrodi, Y.; Pederson, R. L.

DOI: 10.1021/acs.organomet.9b00469
Organometallics XXXX, XXX, XXX−XXX

A Highly Efficient Olefin Metathesis Process for the Synthesis of Terminal Alkenes from Fatty Acid Esters. *Top. Catal.* **2012**, *55*, 518−523. (e) Chikkali, S.; Mecking, S. Refining of Plant Oils to Chemicals by Olefin Metathesis. *Angew. Chem., Int. Ed.* **2012**, *51*, 5802−5808. (f) Mol, J. C. Catalytic Metathesis of Unsaturated Fatty Acid Esters and Oils. *Top. Catal.* **2004**, *27*, 97−104. (g) Burdett, K. A.; Harris, L. D.; Margl, P.; Maughon, B. R.; Mokhtar-Zadeh, T.; Saucier, P. C.; Wasserman, E. P. Renewable Monomer Feedstocks via Olefin Metathesis: Fundamental Mechanistic Studies of Methyl Oleate Ethenolysis with the First-Generation Grubbs Catalyst. *Organometallics* **2004**, *23*, 2027−2047.

(7) (a) *Olefin metathesis of renewable platform chemicals*; de Espinosa, L. M., Meier, M. A. R., Eds.; Springer: Berlin, Heidelberg, 2012. (b) Biermann, U.; Bornscheuer, U.; Meier, M. A. R.; Metzger, J. O.; Schäfer, H. J. Oils and Fats as Renewable Raw Materials in Chemistry. *Angew. Chem., Int. Ed.* **2011**, *50*, 3854−3871. (c) Behr, A.; Gomes, J. P. The Refinement of Renewable Resources: New Important Derivatives of Fatty Acids and Glycerol. *Eur. J. Lipid Sci. Technol.* **2010**, *112*, 31−50. (d) Marshall, A. L.; Alaimo, P. J. Useful Products from Complex Starting Materials: Common Chemicals from Biomass Feedstocks. *Chem. - Eur. J.* **2010**, *16*, 4970−4980. (e) *The Biorefinery Introduction to Chemicals from Biomass*; Clark, J. H., Deswarte, F. E. I., Eds.; Wiley-VCH: Weinheim, Germany, 2008. (f) Behr, A.; Westfechtel, A.; Gomes, J. P. Catalytic Processes for the Technical Use of Natural Fats and Oils. *Chem. Eng. Technol.* **2008**, *31*, 700−714. (g) Clavier, H.; Grela, K.; Kirschning, A.; Mauduit, M.; Nolan, S. P. Sustainable Concepts in Olefin Metathesis. *Angew. Chem., Int. Ed.* **2007**, *46*, 6786−6801. (h) Corma Canos, A.; Iborra, S.; Velty, A. Chemical Routes for the Transformation of Biomass into Chemicals. *Chem. Rev.* **2007**, *107*, 2411−2502. (i) Mol, J. C. Application of Olefin Metathesis in Oleochemistry: An Example of Green Chemistry. *Green Chem.* **2002**, *4*, 5−13.

(8) (a) *Biobased Lubricants and Greases: Technology and Products*; Honary, L. A. T., Richter, E., Eds.; Wiley-VCH: Weinheim, Germany, 2011. (b) *Lubricants and Lubrication*; Mang, T., Drese, W., Eds.; Wiley-VCH: Weinheim, Germany, 2005. (c) Chum, P. S.; Swogger, K. W. Olefin Polymer Technologies-History and Recent Progress at The Dow Chemical Company. *Prog. Polym. Sci.* **2008**, *33*, 797−819.

(9) Ruthenium examples: (a) Engl, P. S.; Santiago, C. B.; Gordon, C. P.; Liao, W. C.; Fedorov, A.; Copéret, C.; Sigman, M. S.; Togni, A. Exploiting and Understanding the Selectivity of Ru-*N*-Heterocyclic Carbene Metathesis Catalysts for the Ethenolysis of Cyclic Olefins to *α,ω*-Dienes. *J. Am. Chem. Soc.* **2017**, *139*, 13117−13125. (b) Engl, P. S.; Fedorov, A.; Copéret, C.; Togni, A. *N*-Trifluoromethyl NHC Ligands Provide Selective Ruthenium Metathesis Catalysts. *Organometallics* **2016**, *35*, 887−893. (c) Miyazaki, H.; Herbert, M. B.; Liu, P.; Dong, X.; Xu, X.; Keitz, B. K.; Ung, T.; Mkrtumyan, G.; Houk, K. N.; Grubbs, R. H. *Z* - Selective Ethenolysis with a Ruthenium Metathesis Catalyst: Experiment and Theory. *J. Am. Chem. Soc.* **2013**, *135*, 5848−5858. (d) Thomas, R. M.; Keitz, B. K.; Champagne, T. M.; Grubbs, R. H. Highly Selective Ruthenium Metathesis Catalysts for Ethenolysis. *J. Am. Chem. Soc.* **2011**, *133*, 7490−7496. (e) Schrodi, Y.; Ung, T.; Vargas, A.; Mkrtumyan, G.; Lee, C. W.; Champagne, T. M.; Pederson, R. L.; Hong, S. H. Ruthenium Olefin Metathesis Catalysts for the Ethenolysis of Renewable Feedstocks. *Clean: Soil, Air, Water* **2008**, *36*, 669−673.

(10) Molybdenum and tungsten examples: (a) Marinescu, S. C.; Levine, D. S.; Zhao, Y.; Schrock, R. R.; Hoveyda, A. H. Isolation of Pure Disubstituted *E* Olefins through Mo-Catalyzed *Z*-Selective Ethenolysis of Stereoisomeric Mixtures. *J. Am. Chem. Soc.* **2011**, *133*, 11512−11514. (b) Marinescu, S. C.; Schrock, R. R.; Müller, P.; Hoveyda, A. H. Ethenolysis Reactions Catalyzed by Imido Alkylidene Monoaryloxide Monopyrrolide (MAP) Complexes of Molybdenum. *J. Am. Chem. Soc.* **2009**, *131*, 10840−10841.

(11) Scholl, M.; Ding, S.; Lee, C. W.; Grubbs, R. H. Synthesis and Activity of a New Generation of Ruthenium-Based Olefin Metathesis Catalysts Coordinated with 1,3-Dimesityl-4,5-dihydroimidazol-2-ylidene Ligands. *Org. Lett.* **1999**, *1*, 953−956.

(12) (a) Kingsbury, J. S.; Harrity, J. P. A.; Bonitatebus, P. J.; Hoveyda, A. H. A Recyclable Ru-Based Metathesis Catalyst. *J. Am. Chem. Soc.* **1999**, *121*, 791−799. (b) Garber, S. B.; Kingsbury, J. S.; Gray, B. L.; Hoveyda, A. H. Efficient and Recyclable Monomeric and Dendritic Ru-Based Metathesis Catalysts. *J. Am. Chem. Soc.* **2000**, *122*, 8168−8179. (c) Gessler, S.; Randl, S.; Blechert, S. Synthesis and metathesis reactions of a phosphine-free dihydroimidazole carbene ruthenium complex. *Tetrahedron Lett.* **2000**, *41*, 9973−9976.

(13) For recent reviews see: (a) Janssen-Müller, D.; Schlepphorst, C.; Glorius, F. Privileged chiral *N*-heterocyclic carbene ligands for asymmetric transition-metal catalysis. *Chem. Soc. Rev.* **2017**, *46*, 4845−4854. (b) Peris, E. Smart *N*-Heterocyclic Carbene Ligands in Catalysis. *Chem. Rev.* **2018**, *118*, 9988−10031. (c) Wang, M. H.; Scheidt, K. A. Cooperative Catalysis and Activation with *N*-Heterocyclic Carbenes. *Angew. Chem., Int. Ed.* **2016**, *55*, 14912−14922. (d) Teator, A. J.; Lastovickova, D. N.; Bielawski, C. W. Switchable Polymerization Catalysts. *Chem. Rev.* **2016**, *116* (4), 1969−1992. (e) Lazreg, F.; Nahra, F.; Cazin, C. S. J. Copper−NHC complexes in catalysis. *Coord. Chem. Rev.* **2015**, *293−294*, 48−79. (f) Flanigan, D. M.; Romanov-Michailidis, F.; White, N. A.; Rovis, T. Organocatalytic Reactions Enabled by *N*-Heterocyclic Carbenes. *Chem. Rev.* **2015**, *115*, 9307−9387. (g) *N-Heterocyclic Carbenes: Effective Tools for Organometallic Synthesis*; Nolan, S. P., Ed.; Wiley-VCH: Weinheim, Germany, 2014. (h) Bellemin-Laponnaz, S.; Dagorne, S. Group 1 and 2 and Early Transition Metal Complexes Bearing *N*-Heterocyclic Carbene Ligands: Coordination Chemistry, Reactivity, and Applications. *Chem. Rev.* **2014**, *114*, 8747−8774. (i) Hopkinson, M. N.; Richter, C.; Schedler, M.; Glorius, F. An overview of *N*-heterocyclic carbenes. *Nature* **2014**, *510*, 485−496. (j) Dröge, T.; Glorius, F. The Measure of All Rings—*N*-Heterocyclic Carbenes. *Angew. Chem., Int. Ed.* **2010**, *49*, 6940−6952. (k) Nolan, S. P.; Marion, N.; Díez-González, S. *N*-Heterocyclic Carbenes in Late Transition Metal Catalysis. *Chem. Rev.* **2009**, *109*, 3612−3676. (l) Kantchev, E. A. B.; O'Brien, C. J.; Organ, M. G. Palladium Complexes of *N*-Heterocyclic Carbenes as Catalysts for Cross-Coupling Reactions—A Synthetic Chemist-s Perspective. *Angew. Chem., Int. Ed.* **2007**, *46*, 2768−2813.

(14) (a) Vougioukalakis, G. C.; Grubbs, R. H. Ruthenium-Based Heterocyclic Carbene-Coordinated Olefin Metathesis Catalysts. *Chem. Rev.* **2010**, *110*, 1746−1787. (b) Samojłowicz, C.; Bieniek, M.; Grela, K. Ruthenium-Based Olefin Metathesis Catalysts Bearing *N*-Heterocyclic Carbene Ligands. *Chem. Rev.* **2009**, *109*, 3708−3742.

(15) (a) Małecki, P.; Gajda, K.; Gajda, R.; Woźniak, K.; Trzaskowski, B.; Kajetanowicz, A.; Grela, K. Specialized Ruthenium Olefin Metathesis Catalysts Bearing Bulky Unsymmetrical NHC Ligands: Computations, Synthesis, and Application. *ACS Catal.* **2019**, *9*, 587−598. (b) Wyrebek, P.; Maecki, P.; Sytniczuk, A.; Kośnik, W.; Gawin, A.; Kostrzewa, J.; Kajetanowicz, A.; Grela, K. Looking for the Noncyclic(Amino)(Alkyl)Carbene Ruthenium Catalyst for Ethenolysis of Ethyl Oleate: Selectivity Is on Target. *ACS Omega* **2018**, *3*, 18481−18488. (c) Paradiso, V.; Bertolasi, V.; Costabile, C.; Caruso, T.; Dąbrowski, M.; Grela, K.; Grisi, F. Expanding the Family of Hoveyda−Grubbs Catalysts Containing Unsymmetrical NHC Ligands. *Organometallics* **2017**, *36*, 3692−3708. (d) Małecki, P.; Gajda, K.; Ablialimov, O.; Malińska, M.; Gajda, R.; Woźniak, K.; Kajetanowicz, A.; Grela, K. Hoveyda−Grubbs-Type Precatalysts with Unsymmetrical *N*-Heterocyclic Carbenes as Effective Catalysts in Olefin Metathesis. *Organometallics* **2017**, *36*, 2153−2166. (e) Hamad, F. B.; Sun, T.; Xiao, S.; Verpoort, F. Olefin metathesis ruthenium catalysts bearing unsymmetrical heterocylic carbenes. *Coord. Chem. Rev.* **2013**, *257*, 2274−2292. (f) Vougioukalakis, G. C.; Grubbs, R. H. Ruthenium Olefin Metathesis Catalysts Bearing an *N*-Fluorophenyl-*N*-Mesityl-Substituted Unsymmetrical *N*-Heterocyclic Carbene. *Organometallics* **2007**, *26*, 2469−2472. (g) Ledoux, N.; Allaert, B.; Pattyn, S.; Mierde, H. V.; Vercaemst, C.; Verpoort, F. *N,N'*-Dialkyl- and *N*-Alkyl-*N*-mesityl-Substituted *N*-Heterocyclic Carbenes as Ligands in Grubbs Catalysts. *Chem. - Eur. J.* **2006**, *12*, 4654−4661. (h) Vehlow, K.; Maechling, S.; Blechert, S. Ruthenium Metathesis Catalysts with

DOI: 10.1021/acs.organomet.9b00469
Organometallics XXXX, XXX, XXX−XXX

Saturated Unsymmetrical *N*-Heterocyclic Carbene Ligands. *Organometallics* **2006**, *25*, 25−28.
(16) Stewart, I. C.; Keitz, B. K.; Kuhn, K. M.; Thomas, R. M.; Grubbs, R. H. Nonproductive Events in Ring-Closing Metathesis Using Ruthenium Catalysts. *J. Am. Chem. Soc.* **2010**, *132*, 8534−8535.
(17) (a) Melaimi, M.; Jazzar, R.; Soleilhavoup, M.; Bertrand, G. Cyclic (Alkyl)(amino)carbenes (CAACs): Recent Developments. *Angew. Chem., Int. Ed.* **2017**, *56*, 10046−10068. (b) Paul, U. S. D.; Radius, U. What Wanzlick Did Not Dare To Dream: Cyclic (Alkyl)(amino)carbenes (cAACs) as New Key Players in Transition-Metal Chemistry. *Eur. J. Inorg. Chem.* **2017**, *2017*, 3362−3375. (c) Roy, S.; Mondal, K. C.; Roesky, H. W. Cyclic Alkyl(amino) Carbene Stabilized Complexes with Low Coordinate Metals of Enduring Nature. *Acc. Chem. Res.* **2016**, *49*, 357−369. (d) Soleilhavoup, M.; Bertrand, G. Cyclic (Alkyl)(Amino)Carbenes (CAACs): Stable Carbenes on the Rise. *Acc. Chem. Res.* **2015**, *48*, 256−266. (e) Melaimi, M.; Soleilhavoup, M.; Bertrand, G. Stable Cyclic Carbenes and Related Species beyond Diaminocarbenes. *Angew. Chem., Int. Ed.* **2010**, *49*, 8810−8849. (f) Lavallo, V.; Canac, Y.; Präsang, C.; Donnadieu, B.; Bertrand, G. Stable Cyclic (Alkyl)(Amino)Carbenes as Rigid or Flexible, Bulky, Electron-Rich Ligands for Transition-Metal Catalysts: AQuaternary Carbon Atom Makes the Difference. *Angew. Chem., Int. Ed.* **2005**, *44*, 5705−5709.
(18) (a) Gawin, R.; Tracz, A.; Chwalba, M.; Kozakiewicz, A.; Trzaskowski, B.; Skowerski, K. Cyclic Alkyl Amino Ruthenium Complexe—Efficient Catalysts for Macrocyclization and Acrylonitrile Cross Metathesis. *ACS Catal.* **2017**, *7*, 5443−5449. (b) Gawin, R.; Kozakiewicz, A.; Guńka, P. A.; Dąbrowski, P.; Skowerski, K. Bis(Cyclic Alkyl Amino Carbene) Ruthenium Complexes: AVersatile, Highly Efficient Tool for Olefin Metathesis. *Angew. Chem., Int. Ed.* **2017**, *56*, 981−986. (c) Butilkov, D.; Frenklah, A.; Rozenberg, I.; Kozuch, S.; Lemcoff, N. G. Highly Selective Olefin Metathesis with CAAC-Containing Ruthenium Benzylidenes. *ACS Catal.* **2017**, *7*, 7634−7637. (d) Zhang, J.; Song, S.; Wang, X.; Jiao, J.; Shi, M. Ruthenium-catalyzed olefin metathesis accelerated by the steric effect of the backbone substituent in cyclic (alkyl)(amino) carbenes. *Chem. Commun.* **2013**, *49*, 9491−9493. (e) Anderson, D. R.; Ung, T.; Mkrtumyan, G.; Bertrand, G.; Grubbs, R. H.; Schrodi, Y. Kinetic Selectivity of Olefin Metathesis Catalysts Bearing Cyclic (Alkyl)-(Amino)Carbenes. *Organometallics* **2008**, *27*, 563−566. (f) Anderson, D. R.; Lavallo, V.; O'Leary, D. J.; Bertrand, G.; Grubbs, R. H. Synthesis and Reactivity of Olefin Metathesis Catalysts Bearing Cyclic (Alkyl)(Amino)Carbenes. *Angew. Chem., Int. Ed.* **2007**, *46*, 7262−7265.
(19) Marx, V. M.; Sullivan, A. H.; Melaimi, M.; Virgil, S. C.; Keitz, B. K.; Weinberger, D. S.; Bertrand, G.; Grubbs, R. H. Cyclic Alkyl Amino Carbene (CAAC) Ruthenium Complexes as Remarkably Active Catalysts for Ethenolysis. *Angew. Chem., Int. Ed.* **2015**, *54*, 1919−1923.
(20) (a) Alder, R. W.; Blake, M. E.; Chaker, L.; Harvey, J. N.; Paolini, F.; Schütz, J. When and how do diaminocarbenes dimerize? *Angew. Chem., Int. Ed.* **2004**, *43*, 5896−5911. (b) Chung, C. K.; Grubbs, R. H. Olefin Metathesis Catalyst: Stabilization Effect of Backbone Substitutions of *N*-Heterocyclic Carbene. *Org. Lett.* **2008**, *10*, 2693−2696.
(21) Alcarazo, M.; Roseblade, S. J.; Cowley, A. R.; Fernández, R.; Brown, J. M.; Lassaletta, J. M. Imidazo[1,5-a]pyridine: A Versatile Architecture for Stable N-Heterocyclic Carbenes. *J. Am. Chem. Soc.* **2005**, *127*, 3290−3291.
(22) Burstein, C.; Lehmann, C. W.; Glorius, F. Imidazo[1,5-a]pyridine-3-ylidenes—pyridine derived N-heterocyclic carbene ligands. *Tetrahedron* **2005**, *61*, 6207−6217.
(23) (a) Park, D. A.; Ryu, J. Y.; Lee, J.; Hong, S. Bifunctional *N*-heterocyclic carbene ligands for Cu-catalyzed direct C−H carboxylation with CO_2. *RSC Adv.* **2017**, *7*, 52496−52502. (b) Tao, W.; Akita, S.; Nakano, R.; Ito, S.; Hoshimoto, Y.; Ogoshi, S.; Nozaki, K. Copolymerisation of ethylene with polar monomers by using palladium catalysts bearing an *N*-heterocyclic carbene−phosphine oxide bidentate ligand. *Chem. Commun.* **2017**, *53*, 2630−2633. (c) Kim, Y.; Kim, Y.; Hur, M. Y.; Lee, E. Efficient synthesis of bulky *N*-Heterocyclic carbene ligands for coinage metal complexes. *J. Organomet. Chem.* **2016**, *820*, 1−7. (d) Nakano, R.; Nozaki, K. Copolymerization of Propylene and Polar Monomers Using Pd/IzQO Catalysts. *J. Am. Chem. Soc.* **2015**, *137*, 10934−10937. (e) Espina, M.; Rivilla, I.; Conde, A.; Díaz-Requejo, M. M.; Pérez, P. J.; Álvarez, E.; Fernández, R.; Lassaletta, J. M. Chiral, Sterically Demanding *N*-Heterocyclic Carbenes Fused into a Heterobiaryl Skeleton: Design, Synthesis, and Structural Analysis. *Organometallics* **2015**, *34*, 1328−1338. (f) Zhang, J. L.; Chen, L. A.; Xu, R. B.; Wang, C. F.; Ruan, Y. P.; Wang, A. E.; Huang, P. Q. Chiral imidazo[1,5-a]-tetrahydroquinoline N-heterocyclic carbenes and their copper complexes for asymmetric catalysis. *Tetrahedron: Asymmetry* **2013**, *24*, 492−498. (g) Francos, J.; Grande-carmona, F.; Faustino, H.; Iglesias-sigu, J.; Díez, E.; Alonso, I.; Ferna, R.; Lassaletta, J. M.; Lo, F.; Mascaren, J. L. Axially Chiral Triazoloisoquinolin-3-ylidene Ligands in Gold(I)-Catalyzed Asymmetric Intermolecular (4 + 2) Cycloadditions of Allenamides and Dienes. *J. Am. Chem. Soc.* **2012**, *134*, 14322−14325. (h) Grohmann, C.; Hashimoto, T.; Fröhlich, R.; Ohki, Y.; Tatsumi, K.; Glorius, F. An Iron(II) Complex of a Diamine-Bridged Bis-*N*-Heterocyclic Carbene. *Organometallics* **2012**, *31*, 8047−8050.
(24) (a) Koto, Y.; Shibahara, F.; Murai, T. Imidazo[1,5-a]pyridin-3-ylidenes as π-accepting carbene ligands: substituent effects on properties of *N*-heterocyclic carbenes. *Org. Biomol. Chem.* **2017**, *15*, 1810−1820. (b) Alcarazo, M.; Stork, T.; Anoop, A.; Thiel, W.; Fürstner, A. Steering the Surprisingly Modular p-Acceptor Properties of N-Heterocyclic Carbenes: Implications for Gold Catalysis. *Angew. Chem., Int. Ed.* **2010**, *49*, 2542−2546. (c) Fürstner, A.; Alcarazo, M.; Krause, H.; Lehmann, C. W. Effective Modulation of the Donor Properties of *N*-Heterocyclic Carbene Ligands by "Through-Space" Communication within a Planar Chiral Scaffold. *J. Am. Chem. Soc.* **2007**, *129*, 12676−12677.
(25) (a) Liu, Z.; Xu, C.; Del Pozo, J.; Torker, S.; Hoveyda, A. H. Ru-Based Catechothiolate Complexes Bearing an Unsaturated NHC Ligand: Effective Cross-Metathesis Catalysts for Synthesis of (*Z*)-α,β-Unsaturated Esters, Carboxylic Acids, and Primary, Secondary, and Weinreb Amides. *J. Am. Chem. Soc.* **2019**, *141*, 7137−7146. (b) Fustero, S.; Simón-Fuentes, A.; Barrio, P.; Haufe, G. Olefin Metathesis Reactions with Fluorinated Substrates, Catalysts, and Solvents. *Chem. Rev.* **2015**, *115*, 871−930. (c) Masoud, S. M.; Mailyan, A. K.; Dorcet, V.; Roisnel, T.; Dixneuf, P. H.; Bruneau, C.; Osipov, S. N. Metathesis Catalysts with Fluorinated Unsymmetrical NHC Ligands. *Organometallics* **2015**, *34*, 2305−2313. (d) Ablialimov, O.; Kedziorek, M.; Malinska, M.; Wozniak, K.; Grela, K. Synthesis, Structure, and Catalytic Activity of New Ruthenium(II) Indenylidene Complexes Bearing Unsymmetrical *N*-Heterocyclic Carbenes. *Organometallics* **2014**, *33*, 2160−2171. (e) Ritter, T.; Day, M. W.; Grubbs, R. H. Rate Acceleration in Olefin Metathesis through a Fluorine-Ruthenium Interaction. *J. Am. Chem. Soc.* **2006**, *128*, 11768−11769. (f) Fürstner, A.; Ackermann, L.; Gabor, B.; Goddard, R.; Lehmann, C. W.; Mynott, R.; Stelzer, F.; Thiel, O. R. Comparative Investigation of Ruthenium-Based Metathesis Catalysts Bearing *N*-Heterocyclic Carbene (NHC) Ligands. *Chem. - Eur. J.* **2001**, *7*, 3236−3253.
(26) (a) Engl, P. S.; Senn, R.; Otth, E.; Togni, A. Synthesis and Characterization of *N*-Trifluoromethyl *N*-Heterocyclic Carbene Ligands and Their Complexes. *Organometallics* **2015**, *34*, 1384−1395. (b) Vougioukalakis, G. C.; Grubbs, R. H. Ruthenium-Based Olefin Metathesis Catalysts Coordinated with Unsymmetrical *N*-Heterocyclic Carbene Ligands: Synthesis, Structure, and Catalytic Activity. *Chem. - Eur. J.* **2008**, *14*, 7545−7556.
(27) Fier, P. S.; Hartwig, J. F. Selective C-H Fluorination of Pyridines and Diazines Inspired by a Classic Amination Reaction. *Science* **2013**, *342*, 956−960.
(28) Hutt, J. T.; Aron, Z. D. Efficient, Single-Step Access to Imidazo[1,5-a]pyridine *N*-Heterocyclic Carbene Precursors. *Org. Lett.* **2011**, *13*, 5256−5259.
(29) (a) Mathew, J.; Koga, N.; Suresh, C. H. C-H Bond Activation through σ-Bond Metathesis and Agostic Interactions: Deactivation

DOI: 10.1021/acs.organomet.9b00469
Organometallics XXXX, XXX, XXX−XXX

Pathway of a Grubbs Second-Generation Catalyst. *Organometallics* **2008**, *27*, 4666−4670. (b) Vehlow, K.; Gessler, S.; Blechert, S. Deactivation of Ruthenium Olefin Metathesis Catalysts through Intramolecular Carbene−Arene Bond Formation. *Angew. Chem., Int. Ed.* **2007**, *46*, 8082−8085. (c) Hong, S. H.; Chlenov, A.; Day, M. W.; Grubbs, R. H. Double C−H Activation of an *N*-Heterocyclic Carbene Ligand in a Ruthenium Olefin Metathesis Catalyst. *Angew. Chem., Int. Ed.* **2007**, *46*, 5148−5151.

(30) (a) Gómez-Suárez, A.; Nelson, D. J.; Nolan, S. P. Quantifying and understanding the steric properties of *N*-heterocyclic carbenes. *Chem. Commun.* **2017**, *53*, 2650−2660. (b) Falivene, L.; Credendino, R.; Poater, A.; Petta, A.; Serra, L.; Oliva, R.; Scarano, V.; Cavallo, L. SambVca 2. A Web Tool for Analyzing Catalytic Pockets with Topographic Steric Maps. *Organometallics* **2016**, *35*, 2286−2293. (c) Nelson, D. J.; Nolan, S. P. Quantifying and understanding the electronic properties of *N*-heterocyclic carbenes. *Chem. Soc. Rev.* **2013**, *42*, 6723. (d) Ragone, F.; Poater, A.; Cavallo, L. Flexibility of *N*-Heterocyclic Carbene Ligands in Ruthenium Complexes Relevant to Olefin Metathesis and Their Impact in the First Coordination Sphere of the Metal. *J. Am. Chem. Soc.* **2010**, *132*, 4249−4258. (e) Clavier, H.; Nolan, S. P. Percent buried volume for phosphine and *N*-heterocyclic carbene ligands: steric properties in organometallic chemistry. *Chem. Commun.* **2010**, *46*, 841−861. (f) Poater, A.; Cosenza, B.; Correa, A.; Giudice, S.; Ragone, F.; Scarano, V.; Cavallo, L. SambVca: A Web Application for the Calculation of the Buried Volume of *N*-Heterocyclic Carbene Ligands. *Eur. J. Inorg. Chem.* **2009**, *2009*, 1759−1766. (g) Hillier, A. C.; Sommer, W. J.; Yong, B. S.; Petersen, J. L.; Cavallo, L.; Nolan, S. P. A Combined Experimental and Theoretical Study Examining the Binding of N-Heterocyclic Carbenes (NHC) to the Cp*RuCl (Cp* = η^5-C_5Me_5) Moiety: Insight into Stereoelectronic Differences between Unsaturated and Saturated NHC Ligands. *Organometallics* **2003**, *22*, 4322−4326.

(31) Computed the Buried Volume of OM Ligands by *SambVca 2.0*. website: https://www.molnac.unisa.it/OMtools/sambvca2.0/index.html (L. Cavallo group. email: luigi.cavallo@kaust.edu.sa).

(32) (a) Huynh, H. V. Electronic Properties of *N*-Heterocyclic Carbenes and Their Experimental Determination. *Chem. Rev.* **2018**, *118*, 9457−9492. (b) Kelly, R. A., III; Clavier, H.; Giudice, S.; Scott, N. M.; Stevens, E. D.; Bordner, J.; Samardjiev, I.; Hoff, C. D.; Cavallo, L.; Nolan, S. P. Determination of N-Heterocyclic Carbene (NHC) Steric and Electronic Parameters using the [(NHC)Ir$(CO)_2$Cl] System. *Organometallics* **2008**, *27*, 202−210.

(33) (a) Verlinden, K.; Buhl, H.; Frank, W.; Ganter, C. Determining the Ligand Properties of N-Heterocyclic Carbenes from ^{77}Se NMR Parameters. *Eur. J. Inorg. Chem.* **2015**, *2015*, 2416−2425. (b) Liske, A.; Verlinden, K.; Buhl, H.; Schaper, K.; Ganter, C. Determining the π-Acceptor Properties of N-Heterocyclic Carbenes by Measuring the ^{77}Se NMR Chemical Shifts of Their Selenium Adducts. *Organometallics* **2013**, *32*, 5269−5272.

(34) (a) Wolf, S.; Plenio, H. On the ethenolysis of end-of-life tire granulates. *Green Chem.* **2013**, *15*, 315−319. (b) Wolf, S.; Plenio, H. On the ethenolysis of natural rubber and squalene. *Green Chem.* **2011**, *13*, 2008−2012.

(35) (a) Engel, J.; Smit, W.; Foscato, M.; Occhipinti, G.; Törnroos, K. W.; Jensen, V. R. Loss and Reformation of Ruthenium Alkylidene: Connecting Olefin Metathesis, Catalyst Deactivation, Regeneration, and Isomerization. *J. Am. Chem. Soc.* **2017**, *139*, 16609−16619. (b) Hong, S. H.; Wenzel, A. G.; Salguero, T. T.; Day, M. W.; Grubbs, R. H. Decomposition of Ruthenium Olefin Metathesis Catalysts. *J. Am. Chem. Soc.* **2007**, *129*, 7961−7968.

DOI: 10.1021/acs.organomet.9b00469
Organometallics XXXX, XXX, XXX−XXX